Modeling the Phase Equilibria of H_2O – CO_2 mixture with PC-SAFT and tPC-PSAFT equations of state

Nikolaos I. Diamantonis[a,b] and Ioannis G. Economou[a,b,*]

[a]*National Center for Scientific Research "Demokritos",*
Institute of Physical Chemistry,
Molecular Thermodynamics and Modelling of Materials Laboratory,
GR–153 10 Aghia Paraskevi Attikis, Greece

[b]*The Petroleum Institute, Department of Chemical Engineering,*
P.O. Box 2533, Abu Dhabi, United Arab Emirates

[*]To whom all correspondence should be addressed at: ieconomou@pi.ac.ae

Abstract

Water – carbon dioxide binary mixture is important for a number of industrial and environmental applications. Accurate modeling of its thermodynamics properties is a challenging task due to the highly non-ideal intermolecular interactions. In this work, two models based on the Statistical Associating Fluid Theory (SAFT) are used to correlate reliable experimental vapor – liquid equilibria (VLE) and liquid – liquid equilibria (LLE) data in the temperature range 298 – 533 K. CO_2 is modeled as a non-associating or associating component within the Perturbed Chain-SAFT (PC-SAFT) and as a quadrupolar component within the truncated PC-Polar SAFT (tPC-PSAFT). It is shown that PC-SAFT with explicit account of H_2O – CO_2 cross-association and tPC-PSAFT with explicit account of CO_2 quadrupolar interactions are the most accurate from the models examined. Saturated liquid mixture density data are accurately predicted by the two models.

Keywords: Carbon capture and storage, water, carbon dioxide transport, equation of state, polar fluids

For publication to *Molecular Physics*

Revised manuscript

December 2011

1. Introduction

Water – carbon dioxide (H_2O – CO_2) mixture is very important for a number of industrial and environmental applications. Being the leading greenhouse gas, CO_2 capture and sequestration has attracted significant attention by scientists and engineers [1]. The most widely accepted approaches to sequester CO_2 are two: either in the beds of deep oceans [2], or in oil reservoirs where the injected CO_2 can act as enhancer for the recovery of oil (enhanced oil recovery – EOR) in the case of a not depleted well [3]. All these processes have a common point that is the continuous appearance of mixtures of CO_2 with other components, such as hydrocarbons, gases, or H_2O [4, 5]. H_2O – CO_2 mixture is also important for CO_2 transport via pipelines, since the flue gas that is transported is not totally dry after the separation processes [6-8]. In addition, in the event of a pipeline rupture, CO_2 immediately mixes with the humidity of the atmosphere. One of the most notable design considerations is that CO_2 is an acid gas and in the presence of H_2O may react to form carbonic acid. The corrosion that stems from the formation of carbonic acid is the main challenge for processes that involve CO_2, something that in oil and gas industry is referred to as “sweet gas” corrosion [9]. Also, the formation of hydrates is potent, under certain conditions [10].

Thermodynamic properties and in particular phase equilibria of H_2O – CO_2 has been studied both experimentally and computationally extensively in the last decades. In most of these approaches, strong intermolecular interactions between H_2O and CO_2 molecules are modeled using an association scheme based on Wertheim’s perturbation theory. Recently, Tsivintzelis et al. [11] modeled the vapor – liquid equilibria (VLE) of the mixture using the cubic plus association (CPA) equation of state (EoS) coupled with two different approaches for the estimation of the cross-association parameters. In the first approach, the arithmetic mean is used for the energy of association and the geometric mean for the volume of association. The second approach uses values from experimental studies that can be found in the literature. They concluded that for CO_2, cross-association with H_2O should be taken into account but self-association should not be included. Also,

due to the high non-ideality of the system, a non-zero binary interaction parameter is required.

Pappa et al. [12] used the Peng-Robinson (PR) EoS in three different variations to study this mixture. Two of them refer to the mixing rules implemented (van der Waals one-fluid and universal mixing rules) and the third approach takes into account the association interactions, using the CPA-PR EoS. In this case, both H_2O and CO_2 are modeled as 4-associating site molecules. This modeling scheme for CO_2 was used by the same group in other studies as well [13, 14]. Their calculations for the solubility of CO_2 in H_2O yield errors less than 25.5 % for temperatures lower than 373 K, while for higher temperatures the maximum error observed was 27.8 %. They concluded that for temperatures lower than 373 K the three models perform similarly. At higher temperatures, the CPA-PR approach is superior over the other two.

The Statistical Associating Fluid Theory (SAFT) theory and its variations (Perturbed Chain-SAFT, etc.) are suitable approaches to model the H_2O – CO_2 mixture. Ji et al. [15] used the SAFT1-RPM EoS, a SAFT-based electrolyte EoS, in order to model H_2O – CO_2 mixture and the effect of NaCl in it. CO_2 was modeled as a 3-associating site molecule. The parameters of energy and volume of cross-association were fitted to experimental data and shown to be temperature dependent, especially for temperatures lower than 373 K. They argue that the temperature dependency of these parameters accounts implicitly for the polar interactions.

Karakatsani et al. [16] used the tPC-PSAFT EoS and modeled CO_2 as a quadrupolar fluid with two sites available only for cross-association with H_2O. H_2O was accounted as 4-sites associating dipolar molecule [17]. A linear temperature dependent binary interaction parameter was used. The non-linear pressure change with composition was very accurately reproduced.

An application of the polar version of PC-SAFT EoS, namely PCP-SAFT, for the same mixture was performed by Tang and Gross [18]. They accounted explicitly for the quadrupole – quadrupole interactions of CO_2, while H_2O was treated as strongly associating component without polar interactions. They reported very good results for

temperatures lower than 373 K, with a temperature dependent binary interaction parameter.

In a recent work, Nguyen-Huynh et al. [19] used the group contribution version of PPC-SAFT. H_2O was modeled as associating dipolar and CO_2 as cross-associating quadrupolar fluid, respectively. The cross-association energy was fitted to experimental data. They obtained relatively high errors for the composition of the phases in equilibrium, relatively higher compared to earlier studies.

The objective of this work is to evaluate thoroughly the accuracy of two PC-SAFT versions, namely the original PC-SAFT and the truncated PC-Polar SAFT (tPC-PSAFT) for modeling the VLE of H_2O – CO_2 mixture. Highly reliable experimental data over a wide temperature range [20-25] are used for this purpose. H_2O is modeled as a 4-associating site component while CO_2 is modeled as either non-associating, associating with different number of sites or polar component. In all cases, a single temperature independent binary interaction parameter is used. It should be mentioned that tPC-PSAFT is more accurate than PC-SAFT in correlating water – hydrocarbon liquid – liquid equilibria (LLE), because of the explicit inclusion of polar interactions [26].

2. Equations of state

The PC-SAFT EoS was developed by Gross and Sadowski [27], and is an extension of the SAFT EoS [28-31]. The theoretical foundations of these models lie on the first order perturbation theory of Wertheim [32-35]. In perturbation theory, the potential energy of a relative complex molecular fluid is described as the sum of the potential energy of a simple reference fluid and a perturbation or correction term. Usually, the first term is known accurately and the challenging part is the description of the perturbation term. If a suitable perturbation term, as a function of temperature, density or pressure, and composition, is developed, then all the remaining thermodynamic properties can be calculated using standard thermodynamic expressions.

In this respect, PC-SAFT EoS is written as a summation of the residual Helmholtz free energy terms that occur due to different types of molecular interactions in the system

under study. The residual Helmholtz free energy is equal to the Helmholtz free energy minus the Helmholtz free energy of the ideal gas at the same temperature T and density ρ.

The exact formalism of Gross and Sadowski [27, 36] was used in this work. For the case of associating term, the elegant formalism of Michelsen and Hendriks [37] was implemented that results in substantial reduction of computing time.

The PC-PSAFT EoS is an extension of PC-SAFT to account explicitly for polar interactions, developed by Karakatsani and Economou [38]. The truncated version of PC-PSAFT (tPC-PSAFT) is a relatively simple, yet accurate, engineering model. Both PC-PSAFT and tPC-PSAFT use the formalism of Larsen et al. [39] for dipolar and quadrupolar interactions. The full development can be found in the work of Karakatsani and Economou [38].

For a system that consists of associating chains, tPC-PSAFT can be expressed as:

$$\frac{A^{res}(T,\rho)}{NRT} = \frac{a^{res}(T,\rho)}{RT} = \frac{a(T,\rho)}{RT} - \frac{a^{ideal}(T,\rho)}{RT} = \frac{a^{ref}(T,\rho)}{RT} - \frac{a^{disp}(T,\rho)}{RT}$$
$$= \frac{a^{hs}(T,\rho)}{RT} + \frac{a^{chain}(T,\rho)}{RT} + \frac{a^{disp}(T,\rho)}{RT} + \frac{a^{assoc}(T,\rho)}{RT} + \frac{a^{polar}(T,\rho)}{RT} + \frac{a^{ind}(T,\rho)}{RT} \quad (1)$$

where a is the Helmholtz free energy per mole and the superscripts res, ideal, ref, hs, chain, disp, assoc, polar and ind refer to residual, ideal, reference, hard sphere (monomer reference fluid), chain, dispersion, association, polar and induced polar interactions respectively. Details on the individual terms can be found in the literature [27, 29, 30, 38].

For an associating component, PC-SAFT requires five parameters that are typically fitted to experimental data, in most cases vapor pressure and saturated liquid density from low temperature up to close to the critical point. These parameters are:

- The number of segments, m, in the chain molecule,
- The chain segment diameter, σ_i,

- The energy of dispersion interactions between segments, ε_i,
- The association energy between sites of like molecules, $\varepsilon^{A_iB_i}$,
- The volume of association interactions, $\kappa^{A_iB_i}$.

For the case of tPC-PSAFT, two additional parameters account for polar interactions:

- The effective polar segment diameter, σ_p, which is fitted to experimental data, and
- The dipole, μ, or quadrupole, Q, moment of the fluid, which is usually measured experimentally.

The models are extended to mixtures using appropriate mixing and combining rules for the various parameters. Dispersion interaction parameters are calculated from Lorentz – Berthelot combining rules [27]:

$$\sigma_{ij} = \frac{1}{2}\left(\sigma_i + \sigma_j\right) \tag{2}$$

$$\varepsilon_{ij} = \left(1 - k_{ij}\right)\sqrt{\varepsilon_i \varepsilon_j} \tag{3}$$

where k_{ij} is a binary interaction parameter fitted to mixture data.

For the association parameters, two approaches were studied in this work. In the first approach, the cross association energy and volume are calculated according to the combining rules proposed by Gross and Sadowski [36]:

$$\varepsilon^{A_iB_j} = \frac{1}{2}\left(\varepsilon^{A_iB_i} + \varepsilon^{A_jB_j}\right) \tag{4}$$

$$\kappa^{A_iB_j} = \sqrt{\kappa^{A_iB_i}\kappa^{A_jB_j}}\left(\frac{\sqrt{\sigma_i\sigma_j}}{\frac{1}{2}\left(\sigma_i + \sigma_j\right)}\right) \tag{5}$$

In the second approach, the energy of cross-association is calculated from Eq. 4, while the volume of cross-association is fitted to mixture VLE experimental data.

3. Results and discussion

PC-SAFT and tPC-PSAFT were initially used for pure H_2O and CO_2 to correlate vapor pressure and saturated liquid density data and calculate the model parameters. Different models were tested for the two components. H_2O was modeled as a 4-associating site molecule (4C in the terminology of Huang and Radosz [30]) with two proton donor and two proton acceptor sites per molecule. This is the most commonly used model for H_2O that has been shown by various researchers [40-45] to provide accurate representation of H_2O and aqueous mixture properties. Model parameters were taken from ref. [46]. In the tPC-PSAFT framework, the dipole – dipole interactions were also taken into account and parameters were taken from ref. [47].

CO_2 was modeled with PC-SAFT as non-associating component and as an associating component with 2 (2B), 3 (3B) or 4 (4C) sites per molecule. In the tPC-PSAFT framework, CO_2 was modeled as a non-associating component with quadrupole – quadrupole interactions. For the case of non-associating CO_2, model parameters were taken from ref. [46] for PC-SAFT and ref. [47] for tPC-PSAFT while for the three associating models, parameters were fitted to experimental vapor pressure and saturated liquid density data [48]. The objective function for the minimization is:

$$O.F. = \min\left[\sum_{i=1}^{N_{data}}\left(\left(\frac{P_i^{EoS}-P_i^{NIST}}{P_i^{NIST}}\right)^2+\left(\frac{\rho_i^{EoS}-\rho_i^{NIST}}{\rho_i^{NIST}}\right)^2\right)\right] \quad (6)$$

In Table 1, the parameter values for the various models and the accuracy in correlating experimental data are shown. Explicit account of dipole – dipole interactions in H_2O results in decrease of the association energy as one might expect. The accuracy in correlating vapor pressure and liquid density increases. Modeling CO_2 as an associating component results in an improvement in the correlation of the vapor pressure but has almost no effect in the correlation of liquid density. The association energy of CO_2 for all three models is significantly lower than the association energy of H_2O and so association in CO_2 is relatively weak. Explicit account of quadrupolar interactions does

not improve the model accuracy in predicting the pure CO_2 vapor pressure and saturated liquid density.

Accurate modeling of H_2O – CO_2 phase equilibria is a challenging task. Experimental data and *ab initio* calculations have revealed strong intermolecular interactions between unlike molecules [49-51]. The carbon atom in CO_2 is considered to behave as a Lewis type electron acceptor, while the oxygen atom in H_2O acts as a Lewis type electron donor. In the PC-SAFT and tPC-PSAFT formalisms, such interactions are modeled using a solvating (cross-associating) scheme. In Table 2, the various schemes used in this work to model H_2O – CO_2 associating interactions are shown. Furthermore, a temperature independent binary interaction parameter (k_{ij} in eq. 3) was fitted to mixture VLE data in the temperature range 298 – 533 K [20-24, 52, 53]. Finally, in approach 2 the cross association volume, $\kappa^{A_iB_j}$, was also fitted to experimental data. In Table 2, k_{ij} and $\kappa^{A_iB_j}$ values for the various models are shown.

The objective function used to calculate the binary interaction parameters is:

$$O.F. = \min\left[\sum_{i=1}^{N_{data}}\left(\left(\frac{K_i^{EoS} - K_i^{exp\,t}}{K_i^{exp\,t}}\right)^2\right)\right] \tag{7}$$

where $K_i = \frac{y_i}{x_i}$ is calculated either from PC-SAFT or tPC-PSAFT based on a TP-flash calculation. In Table 3, the % AAD in the composition of the liquid and vapor phase from the various models is shown. At the lowest temperature examined (298 K), H_2O – CO_2 exhibit VLE at low pressure, while at pressures higher than 6.4 MPa the system exhibits LLE. In this case, the non-associating model for CO_2 (Case 1) provides accurate correlation of the CO_2 solubility in H_2O (Figure 1a) but poor correlation of the H_2O solubility in CO_2 (Figure 1b). The accuracy improves significantly when H_2O – CO_2 solvation is taken into account (Case 2). By making $\kappa^{A_iB_j}$ a second fitted parameter in addition to the k_{ij} parameter (Case 2 – Approach 2), the H_2O solubility correlation improves further, but at the expense of CO_2 solubility. Finally, when CO_2 quadrupole – quadrupole interactions are taken into account, model correlation for both phase solubilities significantly deteriorates (Case 6). In Figures 2 and 3, the H_2O solubility in

CO_2 and CO_2 solubility in H_2O at different temperatures with PC-SAFT (Case 2 – Approach 2) and tPC-PSAFT (Case 6) models are shown. At low temperatures and low pressures, PC-SAFT seems to be more accurate. At temperatures higher than 394 K, calculations from the two models are similar. Calculations from the other models are not presented in detail here, but the overall accuracy of the various approaches can be assessed from Table 3. Clearly, explicit account of association and polar interactions in H_2O (Case 7) results in significant reduction of model accuracy.

An obvious way to increase correlation accuracy is through the introduction of additional adjustable mixture parameters. Ji et al. [15] used SAFT1-PRM and proposed third order polynomials for k_{ij}, the cross association energy and volume with a total of eleven fitted parameters. Excellent correlation was obtained but with limited predictive capability.

Pappa et al. [12] treated used the CPA-PR model with k_{ij} and the cross association energy as linearly dependent on temperature. Moreover, the sets of parameters that they reported are different for the temperature ranges 278 – 373 K and 373 – 623 K, thus requiring a total of eight parameters to be regressed in order to achieve the final results. Tsivintzelis et al. [11] used CPA with two adjustable parameters, that are k_{ij} and a parameter related to cross association volume. In essence, approach 2 here is equivalent to that approach. Tsivintzelis et al. [11] results are similar to the results presented here. In Table 4, a summary of different modeling approaches proposed in the literature are presented for the correlation of H_2O – CO_2 VLE using EoS.

In summary, calculations presented in this work reveal that modeling CO_2 within PC-SAFT as a self-associating component does not improve H_2O – CO_2 VLE and LLE correlation. Instead, by treating CO_2 as solvating component, the model accuracy is improved. For the case of tPC-PSAFT, modeling of CO_2 as quadrupolar fluid results in good correlation of mixture data but it is still less accurate than PC-SAFT.

The optimized models developed here were used to predict the density of H_2O – CO_2 mixture. Experimental data [23, 54] and model predictions from PC-SAFT (Case 2) and

tPC-PSAFT (Case 6) at 298.15 K and 332.15 K are presented in Figure 4. The % AAD is 0.6 % and 0.8 % for PC-SAFT and tPC-PSAFT, respectively.

4. Conclusions

PC-SAFT and tPC-PSAFT equations of state were applied for modeling the VLE of H_2O – CO_2 over an extensive range of temperature and pressure. Several association schemes and polar models were examined for CO_2, while two different approaches to evaluation the cross associating parameters were used. Reliable experimental data were used to validate model calculations.

Pure component parameters were fitted to experimental vapor pressure and saturated liquid density data. Inclusion of dipole – dipole interactions for H_2O improves the accuracy of data correlation. Modeling CO_2 as an associating component provides better correlation of pure component data over modeling it as a quadrupolar fluid.

For mixture calculations, explicit account of H_2O – CO_2 solvation effects through an association scheme clearly improves VLE and LLE correlation. A temperature independent binary interaction parameter is sufficient in all cases. Addition of temperature dependence in this parameter provides a marginal improvement in the calculations. By treating the cross-association volume as a second fitted parameter a marginal improvement in the correlation of experimental data is obtained.

The saturated liquid density of the mixture is predicted accurately by both PC-SAFT and tPC-PSAFT models over a broad pressure range. In summary, PC-SAFT with explicit account of H_2O – CO_2 cross-association and with one adjustable parameter (k_{ij}) is the recommended model for the reliable correlation of mixture phase equilibria.

5. Acknowledgments

The authors acknowledge the financial support of the 7th European Commission Framework Program for Research and Technological Development for the project "Quantitative failure consequence hazard assessment for next generation CO_2 pipelines"

(Project No.: 241346) and from the Petroleum Institute Research Initiation Funding Program for the project “An in-house general-purpose simulator for multiscale multiphase flows in heterogeneous porous media for enhanced oil recovery and carbon capture and storage processes”. Also, The Petroleum Institute is acknowledged for a visiting Ph.D. scholarship to N.I.D.

6. References

1. H. Li and J. Yan, Appl. Energy **86**, 826-836 (2009).
2. C. Marchetti, Climatic Change **1**, 59-68 (1977).
3. T. Holt, J.I. Jensen and E. Lindeberg, Energ. Convers. Manage. **36**, 535-538 (1995).
4. IPCC, IPCC Special Report: Carbon Dioxide Capture and Storage. A Special Report of Working Group III of the Intergovernmental Panel on Climate Change, (2005).
5. S.M. Forbes, P. Verma, T.E. Curry, S.J. Friedmann and S.M. Wade, CCS Guidelines: Guidelines for Carbon Dioxide Capture, Transport, and Storage. World Resources Institute, Washington, DC, (2008).
6. C.B. Wallace, Oil Gas J. **83**, 98-99 (1985).
7. R.M. Ormiston and M.C. Luce, J. Petrol. Technol. **38**, 823-828 (1986).
8. D.N. Nguyen. SPE/EPA/DOE Exploration and Production Environmental Conference, 2003, San Antonio, Texas (2003)
9. J. Barrie, K. Brown, P.R. Hatcher and H.U. Schellhase, *Carbon dioxide pipelines: a preliminary review of design and risk*, in *Greenhouse Gas Control Technologies 7*. 2004: Canada.
10. H. Koide, M. Takahashi, Y. Shindo, Y. Tazaki, M. Iijima, K. Ito, N. Kimura and K. Omata, Energy **22**, 279-283 (1997).
11. I. Tsivintzelis, G.M. Kontogeorgis, M.L. Michelsen and E.H. Stenby, Fluid Phase Equilibr. **306**, 38-56 (2011).
12. G.D. Pappa, C. Perakis, I.N. Tsimpanogiannis and E.C. Voutsas, Fluid Phase Equilibr. **284**, 56-63 (2009).
13. C. Perakis, E. Voutsas, K. Magoulas and D. Tassios, Fluid Phase Equilibr. **243**, 142-150 (2006).
14. C.A. Perakis, E.C. Voutsas, K.G. Magoulas and D.P. Tassios, Ind. Eng. Chem. Res. **46**, 932-938 (2007).
15. X. Ji, S.P. Tan, H. Adidharma and M. Radosz, Ind. Eng. Chem. Res. **44**, 8419-8427 (2005).
16. E.K. Karakatsani, I.G. Economou, M.C. Kroon, M.D. Bermejo, C.J. Peters and G.-J. Witkamp, Phys. Chem. Chem. Phys. **10**, 6160-6168 (2008).
17. M.C. Kroon, E.K. Karakatsani, I.G. Economou, G.-J. Witkamp and C.J. Peters, J. Phys. Chem. B **110**, 9262-9269 (2006).
18. X. Tang and J. Gross, Fluid Phase Equilibr. **293**, 11-21 (2010).
19. D. Nguyen-Huynh, J.-C. de Hemptinne, R. Lugo, J.-P. Passarello and P. Tobaly, Ind. Eng. Chem. Res. **50**, 7467-7483 (2011).
20. R. Wiebe, Chem. Rev. **29**, 475-481 (1941).
21. T. Nakayama, H. Sagara, K. Arai and S. Saito, Fluid Phase Equilibr. **38**, 109-127 (1987).
22. G. Mueller, E. Bender and G. Maurer, Ber. Bunsenges. Phys. Chem. **92**, 148-160 (1988).

23. M.B. King, A. Mubarak, J.D. Kim and T.R. Bott, J. Supercrit. Fluid **5**, 296-302 (1992).
24. A. Bamberger, G. Sieder and G. Maurer, J. Supercrit. Fluid **17**, 97-110 (2000).
25. A. Valtz, A. Chapoy, C. Coquelet, P. Paricaud and D. Richon, Fluid Phase Equilibr. **226**, 333-344 (2004).
26. J. Gross and G. Sadowski, Ind. Eng. Chem. Res. **40**, 1244-1260 (2001).
27. E.K. Karakatsani, G.M. Kontogeorgis and I.G. Economou, Ind. Eng. Chem. Res. **45**, 6063-6074 (2006).
28. W.G. Chapman, K.E. Gubbins, G. Jackson and M. Radosz, Fluid Phase Equilibr. **52**, 31-38 (1989).
29. W.G. Chapman, K.E. Gubbins, G. Jackson and M. Radosz, Ind. Eng. Chem. Res. **29**, 1709-1721 (1990).
30. S.H. Huang and M. Radosz, Ind. Eng. Chem. Res. **29**, 2284-2294 (1990).
31. S.H. Huang and M. Radosz, Ind. Eng. Chem. Res. **30**, 1994-2005 (1991).
32. M.S. Wertheim, J. Stat. Phys. **35**, 19-34 (1984).
33. M.S. Wertheim, J. Stat. Phys. **35**, 35-47 (1984).
34. M.S. Wertheim, J. Stat. Phys. **42**, 459-476 (1986).
35. M.S. Wertheim, J. Stat. Phys. **42**, 477-492 (1986).
36. J. Gross and G. Sadowski, Ind. Eng. Chem. Res. **41**, 5510-5515 (2002).
37. M.L. Michelsen and E.M. Hendriks, Fluid Phase Equilibr. **180**, 165-174 (2001).
38. E.K. Karakatsani and I.G. Economou, J. Phys. Chem. B **110**, 9252-9261 (2006).
39. B. Larsen, J.C. Rasaiah and G. Stell, Mol. Phys. **33**, 987-1027 (1977).
40. T. Kraska and K.E. Gubbins, Ind. Eng. Chem. Res. **35**, 4727-4737 (1996).
41. J.P. Wolbach and S.I. Sandler, Ind. Eng. Chem. Res. **36**, 4041-4051 (1997).
42. E.A. Müller and K.E. Gubbins, Ind. Eng. Chem. Res. **40**, 2193-2211 (2001).
43. C. McCabe, A. Galindo and P.T. Cummings, J. Phys. Chem. B **107**, 12307-12314 (2003).
44. N. von Solms, M.L. Michelsen, C.P. Passos, S.O. Derawi and G.M. Kontogeorgis, Ind. Eng. Chem. Res. **45**, 5368-5374 (2006).
45. G.N.I. Clark, A.J. Haslam, A. Galindo and G. Jackson, Mol. Phys. **104**, 3561 - 3581 (2006).
46. N.I. Diamantonis and I.G. Economou, Energ. Fuel. **25**, 3334-3343 (2011).
47. E.K. Karakatsani and I.G. Economou, Fluid Phase Equilibr. **261**, 265-271 (2007).
48. E.W. Lemmon, M.O. Linden and D.G. Friend, *Thermophysical Properties of Fluid Systems*, in *NIST Chemistry WebBook, NIST Standard Reference Database Number 69*, P.J. Linstrom and W.G. Mallard, Editors, National Institute of Standards and Technology: Gaithersburg MD, 20899.
49. B. Jönsson, G. Karlström and H. Wennerström, Chem. Phys. Lett. **30**, 58-59 (1975).
50. J. Sadlej and P. Mazurek, J. Mol. Struct. THEOCHEM **337**, 129-138 (1995).
51. Y. Danten, T. Tassaing and M. Besnard, J. Phys. Chem. A **109**, 3250-3256 (2005).
52. A. Valtz, C. Coquelet and D. Richon, Int. J. Thermophys. **25**, 1695-1711 (2004).
53. S. Takenouchi and G.C. Kennedy, Am. J. Sci. **262**, 1055-1074 (1964).

54. Z. Li, M. Dong, S. Li and L. Dai, J. Chem. Eng. Data **49**, 1026-1031 (2004).
55. A. Austegard, E. Solbraa, G. De Koeijer and M.J. Mølnvik, Chem. Eng. Res. Des. **84**, 781-794 (2006).
56. R. Wiebe and V.L. Gaddy, J. Am. Chem. Soc. **62**, 815-817 (1940).

TABLES

Table 1. PC-SAFT and tPC-PSAFT parameters for H_2O and CO_2 fitted to vapor pressure and saturated liquid density and % AAD between experimental data and model correlation. Temperature range: 275 – 640 K for H_2O and 217 – 301 K for CO_2.

Component	m	σ (Å)	ε/k (K)	ε^{AB}/k (K)	κ^{AB}	AAD (%)	
						P^{sat}	ρ^{liq}
PC-SAFT							
H2O (4C)	2.1945	2.229	141.66	1804.17	0.2039	1.98	0.83
CO_2 (inert)	2.6037	2.555	151.04	-	-	0.39	0.88
CO_2 (2B)	2.2414	2.713	159.00	512.88	0.0283	0.15	0.92
CO_2 (3B)	2.3056	2.684	156.83	371.15	0.0277	0.13	1.02
CO_2 (4C)	2.2280	2.731	157.25	307.41	0.0287	0.17	1.18
tPC-PSAFT							
H_2O (4C and dipole[a])	2.8150	2.037	150.71	1575.20	0.3518	0.42	0.49
CO_2 (quadrupole[b])	1.9120	2.854	157.97	-	-	0.82	1.04

[a] For H_2O, μ=1.85D , σ_p=3.093 Å and a=1.49 $Å^3$

[b] For CO_2, Q=4.30D and σ_q=2.974 Å.

Table 2. Associating models for H_2O and CO_2, binary interaction parameter values and cross-association volumes. In approach 1, the volume of cross association (κ^{AB}) is calculated from eq. (5) while in approach 2 it is fitted to mixture experimental data. Mixture experimental data in the temperature range 298 – 533 K were used to fit k_{ij} and κ^{AB}.

Case #	**EoS**	**H_2O model**	**CO_2 model**	**Approach 1 (one fitted parameter)**		**Approach 2 (two fitted parameters)**	
				k_{ij}	**κ^{AB}**	**k_{ij}**	**κ^{AB}**
1	PC-SAFT	4C	Non-associating	-0.0033	-	-	-
2	PC-SAFT	4C	Solvating	0.0376	0.1020*	0.0496	0.1435
3	PC-SAFT	4C	2B	0.0986	0.0749	0.0640	0.0604
4	PC-SAFT	4C	3B	0.1217	0.0741	0.0691	0.0537
5	PC-SAFT	4C	4C	0.1174	0.0754	0.0675	0.0425
6	tPC-PSAFT	4C	Non-associating + quadrupole	-0.0286	-	-	-
7	tPC-PSAFT	4C + dipole	Non-associating + quadrupole	0.0107	-	-	-

* This value was set to $\frac{1}{2}\kappa_{H2O}$.

Table 3. % AAD in the correlation of the composition of liquid and vapor phases of H_2O – CO_2 mixture in the temperature range 298 – 533 K from the various models.

Case #	%AAD			
	Approach 1		Approach 2	
	x_{CO2}	y_{H2O}	x_{CO2}	y_{H2O}
1	7.5	37.8	-	-
2	9.7	26.8	10.9	21.6
3	10.3	32.3	9.4	22.0
4	12.0	38.9	10.1	21.7
5	12.7	34.5	10.8	21.7
6	15.0	30.0	-	-
7	17.6	63.2	-	-

Table 4. Summary of literature models for H_2O – CO_2 mixture VLE and reported accuracy.

Model	T [K]	No. of adjustable parameters	%AAD x_{CO2}	%AAD y_{H2O}	Reference
SRK with vdW	243-623	2, for solubility of H_2O in CO_2	93	7.3	[55]
SRK with vdW	243-623	3, for solubility of CO_2 in H_2O	3.5	392	[55]
SRK-Huron Vidal	243-623	7	2.6	7.3	[55]
SRK-Huron Vidal	243-623	5	4	7.5	[55]
SRK-Huron Vidal (Pedersen)	243-623	5	11.6	204	[55]
PR-Henry	278-318	7	2.6	11.7	[25]
PR-Huron Vidal	278-318	3 for every isotherm	4.4	6.4	[25]
UMR-PR	278-373	11	5.6	14	[12]
UMR-PR	373-623	11	12.3	14	[12]
PR	278-373	8	6.2	13.9	[12]
PR	373-623	8	10.1	37.4	[12]
CPA-PR	278-373	8	5.9	9.6	[12]
CPA-PR	373-623	8	7.1	10.3	[12]
CPA (CO_2 as 4C with solvation)	243-623	3	11.8	20.6	[55]
CPA (CO_2 as 4C with solvation)	243-623	3	9	16.8	[55]
CPA (CO_2 as 4C with solvation)	243-623	2	21	28.4	[55]
CPA (CO_2 as 4C with solvation)	243-623	1	43	20.9	[55]
CPA (CO_2 as 4C without solvation)	243-623	0 or 1		56	[55]
CPA (CO_2 as 2B)	298-478	2	16.5	11.9	[11]
CPA (CO_2 as 3B)	298-478	2	12.6	14.7	[11]
CPA (CO_2 as 4C)	298-478	2	10.8	15.1	[11]
SAFT-VR	278-318	2	2.2	12	[25]
GC-PPC-SAFT	298-523	2	41.8	50.1	[19]

FIGURES

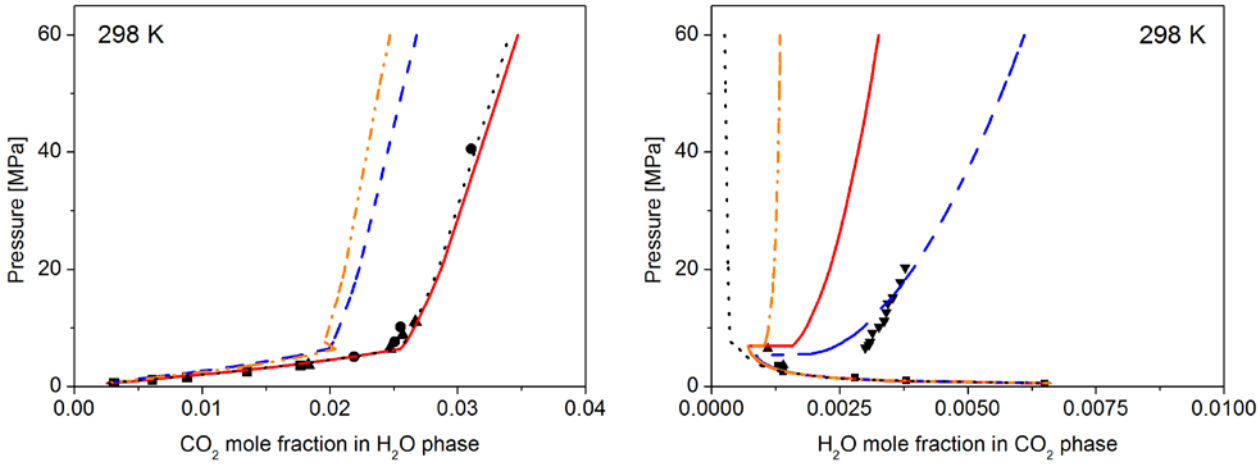

(a) (b)

Figure 1. Pressure – composition diagrams for the H_2O - CO_2 phase equilibria at 298 K: (a) Aqueous phase and (b) CO_2 phase. Experimental data (■ Valtz [25], ● Wiebe [56], ▲ Nakayama [21], ▼ King [23]), and PC-SAFT model correlation using the different association and polar schemes (· · · · Case 1, —— Case 2 – Approach 1, – – – Case 2 – Approach 2, -·-·- Case 6).

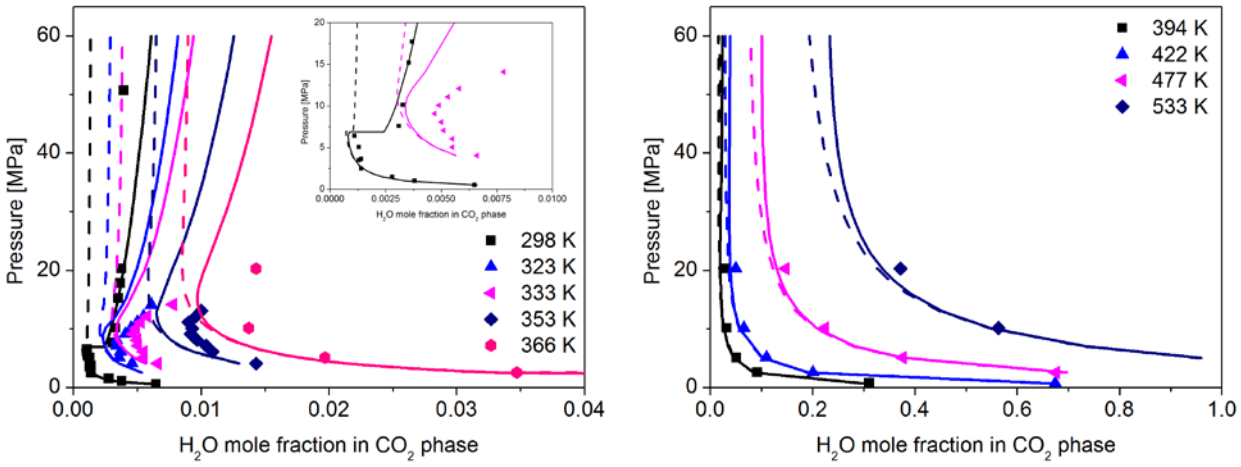

(a) (b)

Figure 2. Pressure – composition diagrams for the H_2O solubility in CO_2 at different temperatures. Experimental data (points), PC-SAFT correlation (solid lines; Case 2 - Approach 2), tPC-PSAFT correlation (dashed lines; Case 6).

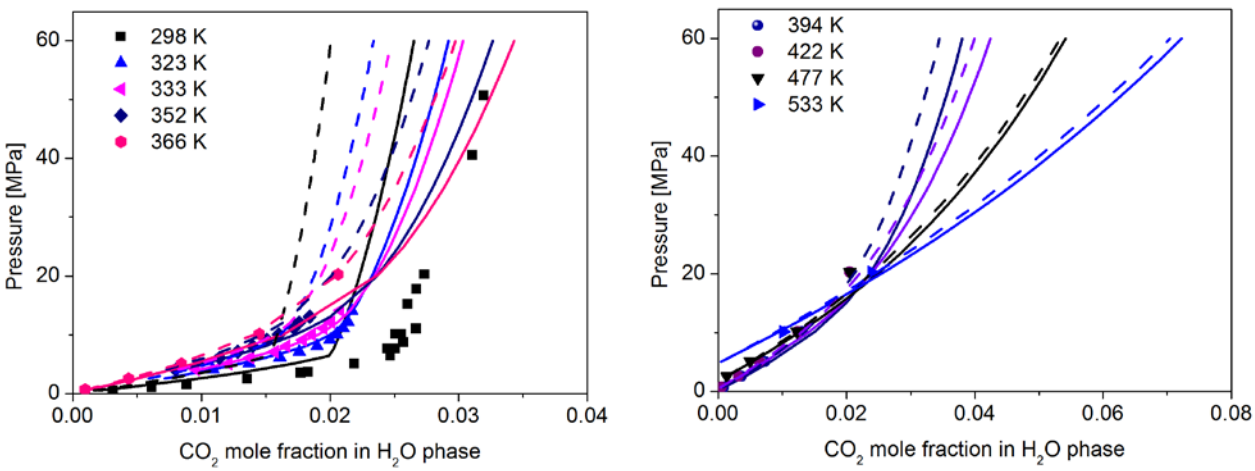

(a) (b)

Figure 3. Pressure – composition diagrams for the CO_2 solubility in H_2O at different temperatures. Experimental data (points), PC-SAFT correlation (solid lines; Case 2 - Approach 2), tPC-PSAFT correlation (dashed lines; Case 6).

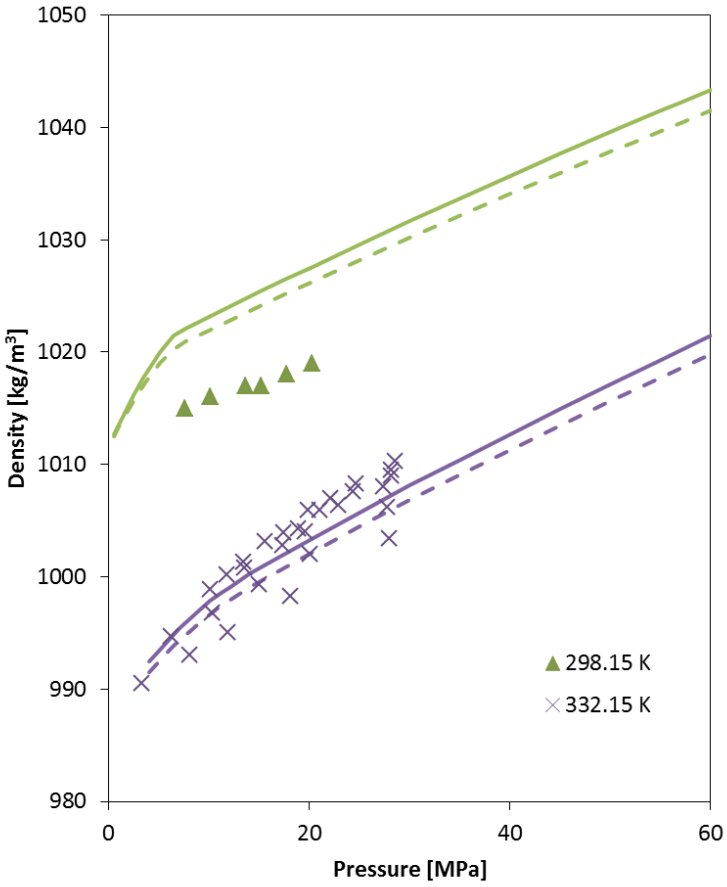

Figure 4. Density of CO_2-saturated H_2O at 298.15 and 332.15 K. Experimental data [23, 53], PC-SAFT prediction (solid lines; Case 2 – Approach 2) and tPC-PSAFT prediction (dashed lines; Case 6).